

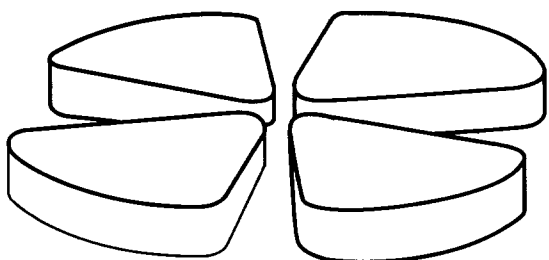
BB

GANIL



SCAN-9508114

CERN LIBRARIES, GENEVA



SW 9533

ELASTIC SCATTERING AND CHARGE EXCHANGE REACTION STUDIES WITH ${}^6\text{He}$, ${}^{10,11}\text{Be}$

M.D. Cortina-Gil¹⁾, P. Roussel-Chomaz¹⁾, N. Alamanos²⁾, J. Barrette³⁾, W. Mittig¹⁾, F. Auger²⁾,
Y. Blumenfeld⁴⁾, J.M. Casandjian¹⁾, M. Chartier¹⁾, V. Fekou-Youmbi²⁾, B. Fernandez²⁾, N.
Frascaria⁴⁾, A. Gillibert²⁾, H. Laurent⁴⁾, A. Lepine^{1,5)}, N.A. Orr⁶⁾, V. Pascalon⁴⁾,
J.A. Scarpaci⁴⁾, J.L. Sida²⁾, T. Suomijärvi⁴⁾

1) GANIL, BP 5027, 14021 Caen Cedex, France

2) CEA/DSM/DAPNIA/SPhN Saclay, 91191 Gif-sur-Yvette Cedex, France

3) Mc Gill University, Montreal, Canada

4) IPN, 91406 Orsay Cedex, France

5) IFUSP,DFN, C.P. 20516, 01498, Sao Paulo, S.P., Brasil

6) LPC-ISMRA, Blvd du Maréchal Juin, 14050 Caen, France

Contribution to ENAM 95, Arles, France

ELASTIC SCATTERING AND CHARGE EXCHANGE REACTION
STUDIES WITH ${}^6\text{He}$, ${}^{10,11}\text{Be}$

M.D. Cortina-Gil¹⁾, P. Roussel-Chomaz¹⁾, N. Alamanos²⁾, J. Barrette³⁾, W. Mittig¹⁾, F. Auger²⁾,
Y. Blumenfeld⁴⁾, J.M. Casandjian¹⁾, M. Chartier¹⁾, V. Fekou-Youmbi²⁾, B. Fernandez²⁾, N.
Frascaria⁴⁾, A. Gillibert²⁾, H. Laurent⁴⁾, A. Lepine^{1,5)}, N.A. Orr⁶⁾, V. Pascalon⁴⁾,
J.A. Scarpaci⁴⁾, J.L. Sida²⁾, T. Suomijärvi⁴⁾

1) GANIL, BP 5027, 14021 Caen Cedex, France

2) CEA/DSM/DAPNIA/SPhN Saclay, 91191 Gif-sur-Yvette Cedex, France

3) Mc Gill University, Montreal, Canada

4) IPN, 91406 Orsay Cedex, France

5) IFUSP,DFN, C.P. 20516, 01498, Sao Paulo, S.P., Brasil

6) LPC-ISMRA, Blvd du Maréchal Juin, 14050 Caen, France

Abstract: We have measured the elastic scattering and charge exchange reaction of ${}^6\text{He}$, ${}^{10,11}\text{Be}$ secondary beams on proton and ${}^{12}\text{C}$ targets. The secondary beams were produced by fragmentation with SISSI, and were transported to SPEG. The combined use of SISSI and SPEG allowed to obtain very good quality data in terms of energy and angular resolution. Preliminary analyses of the angular distributions using global parameter set for the optical model potentials, as well as more microscopic approaches are presented.

Motivations

Elastic scattering measurements provide unique information on the total nuclear matter density distributions¹⁻²⁾, whereas charge exchange reactions connecting the target ground state with its isobaric analog state are sensitive to the difference between the neutron and proton density distributions³⁾. The availability of unstable nuclear beams has created a renewed interest in this type of studies since nuclei with unusually large neutron to proton ratio are predicted to present new type of structure. These investigations should help to better characterize the properties of these exotic nuclear species. They could also allow to test the validity of well established nuclear models which often have been adjusted to reproduce the properties of stable or nearly stable nuclei close to the stability valley.

We have commenced at GANIL an experimental programme for the study of elastic, inelastic and charge-exchange reactions induced by light unstable nuclei. These experiments benefit from the high resolution energy loss spectrometer SPEG and from the high quality secondary beams that are provided using the double superconducting solenoid SISSI⁴⁾. We report here on some of the results

of the first experiment of this programme, where we were interested in light neutron rich-nuclei, in particular, ${}^6\text{He}$ and ${}^{10,11}\text{Be}$.

Experimental methods

The secondary beams were produced by fragmentation of a 75 MeV/nucleon primary ${}^{13}\text{C}$ beam, delivered by the GANIL accelerator, on a 1155 mg/cm^2 carbon production target, located between the two superconducting solenoids of SISSI. The position of SISSI at the exit of the second cyclotron and at the entrance of the beam analysing α -spectrometer allows for an improved collection of secondary beams and transmission to the different experimental areas. The momentum acceptance of the system SISSI+ α -spectrometer was of the order of 0.6% and the angular acceptance was around 100 mrad in the horizontal and vertical directions. This results in roughly one order of magnitude increase in beam intensity.

The total intensity of the secondary beam was of the order of 10^7 particles/second for a primary intensity of 2×10^{12} particles/second. The intensity for the more neutron rich nuclei ${}^6\text{He}$ and ${}^{11}\text{Be}$ was of the order of a few percent of the total intensity, whereas the intensity for the nuclei closer to the stability valley such as ${}^7\text{Li}$ and ${}^{10}\text{Be}$ were around 15 or 20% of the total intensity. We ran the experiment with the composite beam (instead of using an achromatic degrader to purify the secondary beam) in order to avoid any additional increase of the emittance and any additional loss of intensity for the most neutron-rich fragments.

The secondary reaction target was a foil of $100\mu\text{m}$ thick polypropylene, $(\text{CH}_2)_3$. The scattered particles were identified in the focal plane of SPEG by the energy-loss measured in an ionisation chamber and the residual energy measured in a plastic scintillator. All the fragments could thus be unambiguously identified. The momentum and scattering angle were obtained by track reconstruction of the trajectory as determined by two drift chambers placed 70 cm apart and located near the focal plane of the spectrometer. The elastic and inelastic scattering of the secondary beam were measured on ${}^1\text{H}$, ${}^{12}\text{C}$, and ${}^{208}\text{Pb}$ targets in the range $\theta_{\text{lab}}=0.7^\circ$ - 6.0° , while the charge exchange reactions on ${}^1\text{H}$ and ${}^{12}\text{C}$ were obtained from $\theta_{\text{lab}}=0.0^\circ$ to 4.0° .

Elastic scattering on protons

Figure 1 shows a typical momentum spectrum for 60 MeV/nucleon ${}^{10}\text{Be}$ scattered on a $(\text{CH}_2)_3$ target. The different peaks correspond, from right to left (decreasing momentum) to the elastic scattering of ${}^{10}\text{Be}$ on ${}^{12}\text{C}$, to the inelastic scattering on the first excited state in ${}^{12}\text{C}$ at 4.4 MeV, and finally to the elastic scattering on the protons in the target. The broad structure underneath the ${}^{12}\text{C}$ inelastic peak corresponds to the excitation of the first excited state in ${}^{10}\text{Be}$ at 3.37 MeV which is broadened due to in-flight γ decay. The energy resolution (FWHM) deduced from the elastic scattering on ${}^{12}\text{C}$ is of the order $\Delta E/E=10^{-3}$, and the angular resolution, which is mainly determined by the angular width of the incident secondary beam is $\Delta\theta_{\text{lab}}=0.3^\circ$. These results are quite unique: for the first time a clear separation between elastic and inelastic scattering is obtained in experiments involving unstable projectiles produced by nuclear fragmentation.

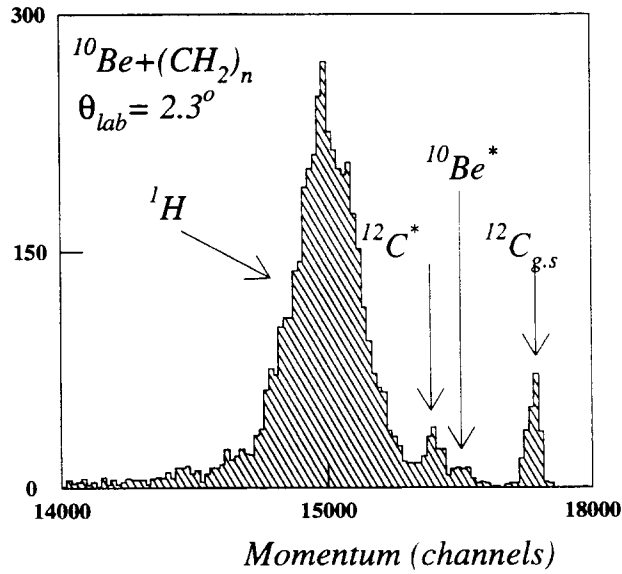


Fig.1: Momentum spectrum measured at $\Theta_{lab}=2.8^\circ$ for the $^{10}\text{Be}+(\text{CH}_2)_3$ reaction at 59.3 MeV/nucleon

- i) the potential obtained for the system ^{12}Be on ^{12}C at 56.7 MeV/nucleon⁶), (solid line)
- ii) the potential obtained for the system ^{16}O on ^{12}C at 95 MeV/nucleon⁷), (dashed line)
- iii) the parametrisation of the optical model potential derived par A. Winther and R. Broglia at low energy⁸), (dotted line).

This figure illustrates the fact that for the very forward angles measured in the present experiment, the calculated angular distributions do not depend on the nuclear interaction potential, and that the normalisation of the data can be obtained very precisely from the value on the first maximum of the angular distribution. We estimate the uncertainty on this absolute normalisation around 10% for all the systems.

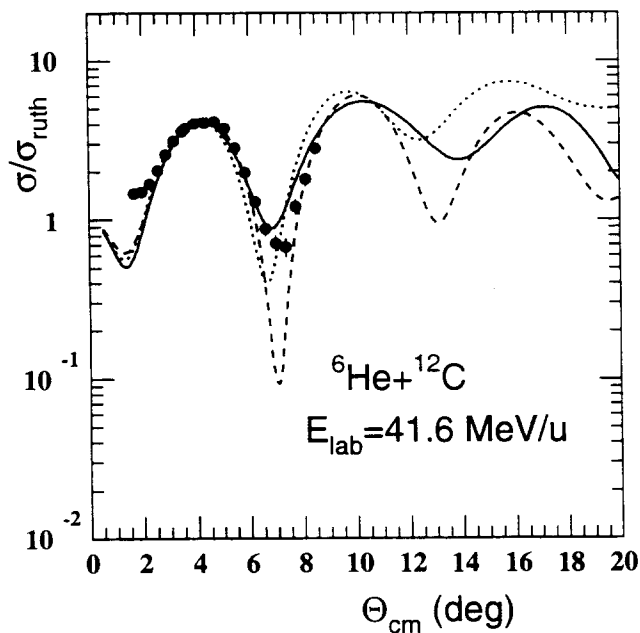


Fig. 2: Elastic scattering angular distribution for $^6\text{He}+^{12}\text{C}$ at 41.6 MeV/nucleon

As we did not measure the number of incident particles on the target in this experiment, it was not possible to obtain the absolute normalisation in a direct way. Instead, the absolute normalisation was obtained from the elastic scattering of the different secondary beams on the ^{12}C atoms of the $(\text{CH}_2)_3$ target, which was measured simultaneously. Figure 2 presents the angular distribution measured for elastic scattering of ^6He on ^{12}C , compared to different calculations performed with arbitrary optical model potentials:

i) the potential obtained for the system ^{12}Be on ^{12}C at 56.7 MeV/nucleon⁶), (solid line)

ii) the potential obtained for the system ^{16}O on ^{12}C at 95 MeV/nucleon⁷), (dashed line)

iii) the parametrisation of the optical model potential derived par A. Winther and R. Broglia at low energy⁸), (dotted line).

The experimental angular distributions measured for the scattering of ^6He , ^7Li , $^{10,11}\text{Be}$ secondary beams on the protons in the $(\text{CH}_2)_3$ target are presented in Figure 3. The elastic scattering of ^7Li on proton had been measured previously at 65 MeV/nucleon⁹). We have checked that the angular distribution measured for this system in the present experiment and the one reported by C.B. Moon et al. are very similar (within a few percent). We have first analysed these data by using standard parametrisation of the nucleon-nucleus optical model potential. We have used the parameters of Becchetti and Greenlees¹⁰) (BG, dotted lines on the figure) and the so-called CH89 parameters¹¹)

(dashed line). As could be expected from the fact that the CH89 parametrisation was obtained from a more complete and accurate set of data, this parametrisation provides angular distributions which lie closer to the data than the ones calculated with the BG parameters. It should be noted that these kind of parametrisations were adjusted to data for nuclei in the mass range $A=40-209$. Therefore the excellent fit obtained for ${}^7\text{Li}$ is rather remarkable and shows that the CH89 potential gives good results also for very light nuclei close to the stability valley. However, in the case of the neutron rich nuclei ${}^6\text{He}$ and ${}^{10,11}\text{Be}$, the calculated angular distributions lie significantly above the data. Furthermore, in the case of ${}^{11}\text{Be}$, the structure around $\Theta_{\text{cm}} \approx 45^\circ$ is much more attenuated in our data than predicted by the calculations. For these neutron-rich nuclei, it was possible to obtain good fits of the data by adjusting the parameters of the volume imaginary component of the CH89 potential. However considering the rather restricted angular range covered by our data, we did not try, for the present time, to draw conclusions concerning the modification of the imaginary potential shape.

We also calculated the angular distributions in a more microscopic approach, by using the potential derived by J.P. Jeukenne, A. Lejeune and C. Mahaux (JLM)¹²⁾, which has been particularly successful in describing neutron and proton scattering from stable nuclei, provided the imaginary is adjusted downward by 20%. The results is presented by the solid line in Fig. 3 and lies very close to

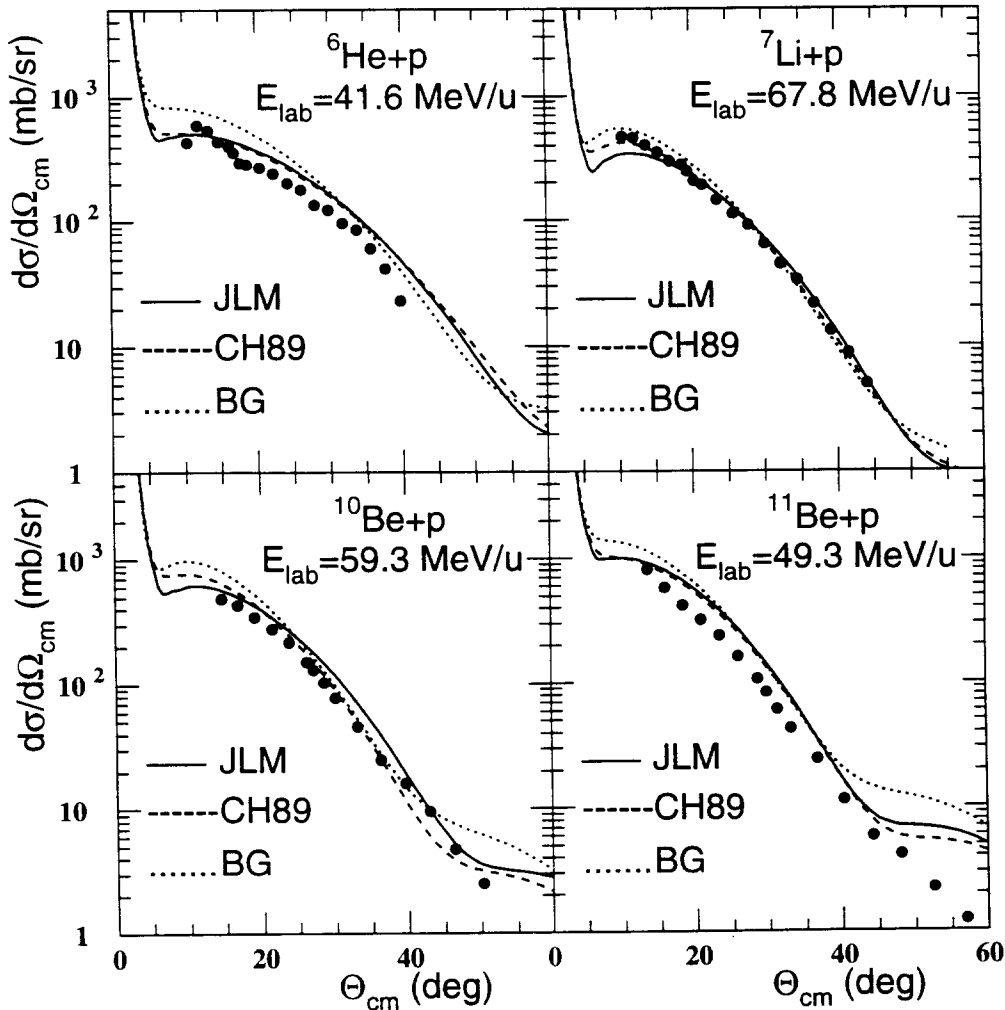


Fig 3: Elastic scattering angular distributions for ${}^6\text{He}$, ${}^7\text{Li}$, ${}^{10}\text{Be}$ and ${}^{11}\text{Be} + {}^1\text{H}$

the angular distribution calculated with the CH89 potential. The next step will be to test how the calculated angular distributions are sensitive to the normalisation of the imaginary potential or to the density distribution which enters in the folding procedure.

${}^6\text{He}(p,n){}^6\text{Li}$ charge exchange reaction

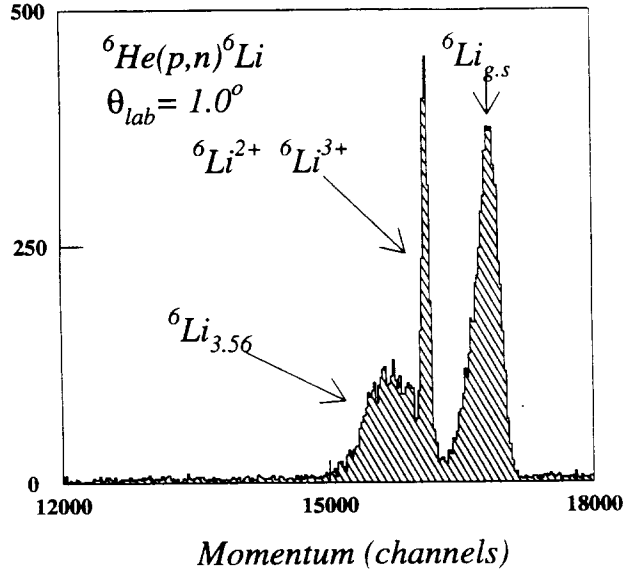


Fig.4: Momentum spectrum for the ${}^6\text{He}(p,n){}^6\text{Li}$ reaction measured at $\Theta_{\text{lab}}=1^\circ$ with $\Delta\Theta_{\text{lab}}=1^\circ$

The absolute normalisation for the angular distributions for the ${}^6\text{He}(p,n){}^6\text{Li}_{\text{GS}}$ and ${}^6\text{Li}_{3.56\text{MeV}}$ reactions was obtained through the detailed balance principle, from the inverse reaction ${}^6\text{Li}(n,p){}^6\text{He}$, for which extensive data exist¹³):

$$\sigma_{{}^6\text{He}(p,n){}^6\text{Li}_{\text{GS}}} = 3 \times \sigma_{{}^6\text{Li}(n,p){}^6\text{He}}$$

The angular distributions are presented in Figure 5. They are very similar in shape and the ratio between the cross sections for ${}^6\text{He}(p,n){}^6\text{Li}_{\text{GS}}$ and ${}^6\text{Li}_{3.56}$ is 1.7. The curves correspond to calculations performed with ECIS with the BG (dashed line) and CH89 (solid line) parametrisation of the proton-nucleus and neutron-nucleus potentials, for the IAS transition. The transition form factor for

the charge exchange leading to the IAS of the ${}^6\text{He}$ ground state, was estimated following the prescription of Lane¹⁴). Apart from the fact that both calculations overestimate the measured cross

A momentum spectrum obtained for the reaction ${}^6\text{He}(p,n){}^6\text{Li}$ at $\theta_{\text{lab}}=1^\circ$, with $\Delta\theta=1^\circ$, is shown in figure 4. The narrow peak in the middle of the spectrum corresponds to the stripping in the target of the secondary beam ${}^6\text{Li}^{2+}$ to ${}^6\text{Li}^{3+}$. This peak provides a direct information on the angular width of the beam, which for the (p,n) measurements was of the order of 1° . The other peaks correspond, from right to the left, to the (p,n) reaction populating the ground state and the 3.56 MeV state of ${}^6\text{Li}$. The latter is the isobaric analog state of the ${}^6\text{He}$ ground state and its study was one of the main motivations for the present experiment.

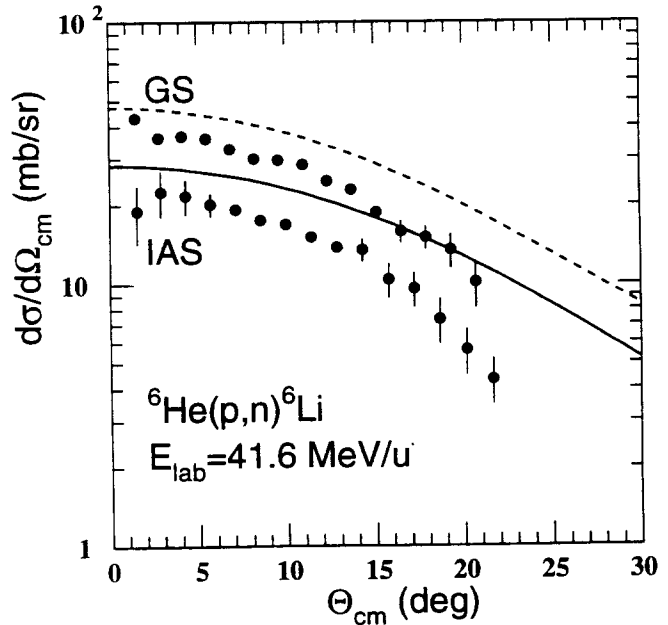


Fig.5: Angular distribution for the ${}^6\text{He}(p,n){}^6\text{Li}_{\text{GS}}$ and ${}^6\text{He}(p,n){}^6\text{Li}_{3.56\text{MeV}}$ reactions

section, the striking feature is the difference in shape between the calculated angular distribution and the data, for angles larger than 15° . In the case of the CH89 potential, a reduction by 30% of the real amplitude of the transition term was sufficient to remove the discrepancy in absolute value at forward angle. However the difference in shape at larger angle is as yet, not understood. As the transition to the IAS is sensitive to the difference between the neutron and proton distributions, we expect that the analysis of these measurements in the framework of microscopic calculations, will provide additional information on these features of exotic nuclei.

Conclusions and outlook

In summary, we have shown that the combined use of SISSI and SPEG offers new opportunities for reaction studies which lead, in particular, to discrete states. Concerning the elastic scattering, the results obtained in this first experiment cover an angular range which may be too restricted to allow us to draw conclusions on the evolution of the nuclear interaction potential, but will already help us to identify general trends. Another experiment is planned in order to measure the angular distributions of elastic scattering for the Be isotopes on proton, ^{12}C , and ^{208}Pb on a wider angular range. The analysis of the $^6\text{He}(p,n)^6\text{Li}$ charge exchange reactions with standard interaction and transition potentials have shown that several features of the data cannot be reproduced. Work is still in progress in order to compare these data with distorted wave calculations using shell model wave functions and the effective nucleon-nucleon interaction of Love and Franey. The combined analysis of the elastic, $^6\text{He}(p,p)^6\text{He}$, and the charge exchange reaction, $^6\text{He}(p,n)^6\text{Li}$, which connects the target ground state with its isobaric analog state, should help to better determine the neutron density distribution of this neutron rich nucleus.

References

- 1) F. Petrovich et al., *Ann. Rev. Nucl. Part. Sci.* 36 (1986) 29.
- 2) R. Satchler and W. G. Love *Phys. Rep.* 55 (1979) 183.
- 3) C. J. Batty et al., *Adv. Nucl. Phys.* 19 (1989) 1.
- 4) A. Joubert et al., 1991 Particle Accelerator Conference IEEE Vol 1 (1991) 594
- 5) H. Laurent et al, *Nucl. Inst. and Meth.* A326 (1993) 517
- 6) M. Zahar et al., *Phys. Rev.* C49 (1994) 1540
- 7) P. Roussel-Chomaz et al., *Nucl. Phys.* A477 (1988) 345
- 8) R. A. Broglia and A. Winther, *Heavy ion reactions*, Vol 1, (Benjamin Cummings, Reading, MA)
- 9) C.B. Moon et al., *Phys. Lett.* B297 (1992) 39
- 10) F.D. Bechetti and G.W. Greenlees, *Phys. Rev.* 182 (1969) 1190
- 11) R.L. Varner et al., *Phys. Rep.* 201 (1991) 57
- 12) J.P. Jeukenne, A.Lejeune and C. Mahaux, *Phys. Rev.* C16 (1977) 80
- 13) D.S. Sorenson et al, *Phys. Rev.* C45 (1992) R500
- 14) A.M. Lane, *Nucl. Phys.* 35 (1962) 676